Research in Astron. Astrophys. **2009** Vol. **9** No. **5**, 547 – 557
http://www.raa-journal.org *http://www.iop.org/journals/raa*

***R**esearch in*
***A**stronomy and*
***A**strophysics*

Constraints on generalized Chaplygin gas model including gamma-ray bursts *

Fa-Yin Wang[1], Zi-Gao Dai[1] and Shi Qi[2,3]

[1] Department of Astronomy, Nanjing University, Nanjing 210093, China; *fayinwang@nju.edu.cn; dzg@nju.edu.cn*
[2] Purple Mountain Observatory, Chinese Academy of Sciences, Nanjing 210008, China
[3] Joint Center for Particle, Nuclear Physics and Cosmology, Nanjing University - Purple Mountain Observatory, Nanjing 210093, China

Received 2008 June 8; accepted 2008 December 11

Abstract Generalized Chaplygin gas (whose equation of state is $p_{\rm GCG} = -A/\rho^{\alpha}_{\rm GCG}$) was proposed as a candidate for unification of dark energy and dark matter. We investigate constraints on this model with the latest observed data. We test the model with type-Ia supernovae (SNe Ia), cosmic microwave background (CMB) anisotropy, X-ray gas mass fractions in clusters, and gamma-ray bursts (GRBs). We calibrate the GRB luminosity relations without assuming any cosmological models using SNe Ia. We show that GRBs can extend the Hubble diagram to higher redshifts ($z > 6$). The GRB Hubble diagram is well behaved and delineates the shape of the Hubble diagram well. We measure $A_s \equiv A/\rho^{\alpha+1}_{\rm GCG,0} = 0.68^{+0.04}_{-0.08}$ (where $\rho_{\rm GCG,0}$ is the energy density today) and $\alpha = -0.22^{+0.15}_{-0.13}$ at the 1σ confidence level using all the datasets. Our results rule out the standard Chaplygin gas model ($\alpha = 1$) at the 3σ confidence level. The ΛCDM is allowed at the 2σ confidence level. We find that acceleration could have started at a redshift of $z \sim 0.70$. The concordance of the generalized Chaplygin gas model with the age estimate of an old high redshift quasar is found. In addition, we show that GRBs can break the degeneracy between the generalized Chaplygin gas model and the XCDM model.

Key words: gamma-rays: bursts — cosmology: theory

1 INTRODUCTION

Observations of type Ia supernovae (SNe Ia) indicate that the universe is experiencing an accelerated expansion during the present epoch (Riess et al. 1998; Perlmutter et al. 1999). The cosmic accelerated expansion has also been confirmed by observations of cosmic microwave background (CMB) fluctuations (Bennett et al. 2003; Spergel et al. 2003, 2007; Komatsu et al. 2008), and large-scale structure (LSS) (Tegmark et al. 2006). These observations suggest that the composition of the universe may consist of an extra component such as dark energy. A possible candidate responsible for this component is the vacuum energy represented by a cosmological constant Λ which has negative pressure (Weinberg 1989; Peebles & Ratra 2003). However, fine tuning is required to make the cosmological constant energy density dominant at the recent epoch. Many other candidates for dark energy have also been proposed in the literature, e.g., quintessence (Wetterich 1988; Ratra & Peebles 1988; Caldwell, Dave & Steinhardt 1998), extra-dimension motivated models (Dvali, Gabadadze & Porrati 2000; Deffayet, Dvali & Gabadadze

* Supported by the National Natural Science Foundation of China.

2002; Zhu & Fujimoto 2002), holographic dark energy (Cohen, Kaplan & Nelson 1999; Li 2004), and so on. Unfortunately, dark energy and dark matter have no direct laboratory evidence for their existence. In this regard, Chaplygin gas has recently been suggested as a model for unifying dark matter and dark energy (Kamenshchik, Moschella & Pasquier 2001; Bento et al. 2002).

The Chaplygin gas has an exotic equation of state

$$p_{\rm Ch} = -A/\rho_{\rm Ch}, \tag{1}$$

where A is a positive constant. Using the above expression, one can solve the conservation of energy equation in a Robertson-Walker metric to obtain

$$\rho_{\rm Ch} = \sqrt{A + \frac{B}{a^6}}, \tag{2}$$

where B is an integration constant and a is the scale factor of the universe. The attractive feature of the model is that it can unify dark energy and dark matter. The reason for this is that, from Equation (2), the Chaplygin gas behaves as dustlike matter during an early epoch and as a cosmological constant in a later epoch. It is interesting that the Chaplygin gas can be derived from the quintessence Lagrangian for the scalar field with some potential and also from the Born-Infeld form of the Lagrangian (Kamenshchik, Moschella & Pasquier 2001). Recently, Bento et al. (2002) generalized the original Chaplygin gas model. The equation of state of the generalized Chaplygin gas (GCG) is

$$p_{\rm GCG} = -A/\rho^{\alpha}_{\rm GCG}. \tag{3}$$

A lot of work related to observational constraints in the GCG model has been done (Multamaki, Manera & Gaztanaga 2004; Wu & Yu 2007; Guo & Zhang 2007). The GCG model has been successfully validated with various phenomenological tests: SNe Ia data (Makler, de Oliveira & Waga 2003; Bertolami et al. 2004; Gong & Duan 2004), CMB (Bento, Bertolami & Sen 2003), gravitational lensing (Dev, Jain & Alcaniz 2003; Silva & Bertolami 2003), dimensionless coordinate distances to SNe Ia and distant FRIIb radio galaxies (Zhu 2004), X-ray gas mass fraction in clusters (Zhu 2004), and gamma-ray bursts (GRBs) (Bertolami & Silva 2006). More recently, an interacting Chaplygin gas model was proposed as a possible mechanism for acceleration (Zhang & Zhu 2006).

GRBs could provide a complementary probe of cosmic expansion and dark energy. Recently, some luminosity calibrators were used to constrain cosmological parameters and the nature of dark energy (Dai, Liang & Xu 2004; Ghirlanda et al. 2004; Di Girolamo et al. 2005; Firmani et al. 2005; Friedman & Bloom 2005; Lamb et al. 2005; Liang & Zhang 2005, 2006; Xu, Dai & Liang 2005; Wang & Dai 2006; Schaefer 2007; Wright 2007; Wang, Dai & Zhu 2007; Gong & Chen 2007; Li et al. 2007; Li et al. 2008; Liang et al. 2008; Qi, Wang & Lu 2008a,b; Amati et al. 2008; Basilakos & Perivolaropoulos 2008). Very recently, Schaefer (2007) used 69 GRBs together with five relations to extend the Hubble diagram out to $z = 6.60$ and discussed properties of dark energy in several models. He found that the GRB Hubble diagram is consistent with the concordance cosmology. Wang, Dai & Zhu (2007) combined GRBs with other cosmological probes and found that for the ΛCDM model, this combination makes the constraints more stringent.

In this paper, we calibrate the GRB luminosity relations without assuming any cosmological models using SNe Ia and measure model parameters of GCG using GRBs, SNe Ia, CMB shift parameter and X-ray gas mass fraction in clusters. The structure of this paper is arranged as follows: in Section 2, we give a brief description of the GCG model and its basic equations. In Section 3, we calibrate the GRB luminosity relations and introduce the observational data and analytical method. In Section 4, we investigate constraints on GCG parameters using the latest observational datasets and apply an age test to the GCG model. In Section 5, we calculate the snap parameter and find that GRBs can break the degeneracy between the GCG model and XCDM model. In Section 6, our conclusions are summarized.

2 BASIC EQUATIONS OF GCG

Assuming a flat universe that contains only baryonic matter and GCG as a unification of dark energy and dark matter, the Friedmann equation can be expressed by

$$H^2 = \frac{8\pi G}{3}(\rho_{\rm b} + \rho_{\rm GCG}). \tag{4}$$

If we further assume that these two components do not interact, then the energy conservation equation becomes

$$\dot{\rho} + 3H(p + \rho) = 0, \tag{5}$$

where $H = \dot{a}/a$ is the Hubble function. We can separately integrate baryonic matter and GCG, leading to $\rho_{\rm b} = \rho_{\rm b,0} a^{-3}$ and

$$\rho_{\rm GCG} = \rho_{\rm GCG,0}[A_s + (1 - A_s)a^{-3(1+\alpha)}]^{1/(1+\alpha)} \tag{6}$$

where $\rho_{\rm b,0}$ and $\rho_{\rm GCG,0}$ are the energy densities of baryonic matter and GCG today, respectively, and $A_s = A/\rho^{1+\alpha}_{\rm GCG,0}$. From the above equation, we can see that A_s must lie in the range $0 \leq A_s \leq 1$, and for $A_s = 0$, the GCG behaves like matter, while for $A_s = 1$, it always behaves like the cosmological constant. We consider GCG as a unification of dark energy and dark matter, so $0 < A_s < 1$. The Friedmann equation can be further expressed as

$$H^2(z, H_0, A_s, \alpha) = H_0^2 E^2(z, A_s, \alpha), \tag{7}$$

where

$$E^2(z, A_s, \alpha) = \Omega_{\rm b}(1 + z)^3 + (1 - \Omega_{\rm b})[A_s + (1 - A_s)(1 + z)^{3(1+\alpha)}]^{\frac{1}{1+\alpha}}, \tag{8}$$

$\Omega_{\rm b}$ is the density parameter of baryonic matter and $H_0 = 100h\,{\rm km\,s^{-1}\,Mpc^{-1}}$ is the present Hubble constant. We use $h = 0.72 \pm 0.08$ from the *Hubble Space Telescope key projects* (Freedman et al. 2001) and $\Omega_{\rm b}h^2 = 0.0214 \pm 0.0020$ (Kirkman et al. 2003). In the GCG model, the luminosity distance for a flat universe is

$$d_{\rm L} = cH_0^{-1}(1 + z)\int_0^z dz\{(1 + z)^3\Omega_{\rm b} + (1 - \Omega_{\rm b})[A_s + (1 - A_s)(1 + z)^{3(1+\alpha)}]^{\frac{1}{1+\alpha}}\}^{-1/2}. \tag{9}$$

3 OBSERVATIONAL DATA AND ANALYSIS METHODS

3.1 Gamma-Ray Bursts (GRBs)

We use 192 SNe Ia from Davis et al. (2007). Because the minimum redshift of 69 GRBs is $z = 0.1685$, we select SNe Ia between $0.159 < z < 1.39$. We exclude SN 1977ff ($z = 1.775$) only because this SN is in the redshift bin $1.40 - 1.755$. There are 146 SNe Ia in our sample. We fit the formula between luminosity distance and redshift as:

$$\frac{d_{\rm L}}{10^{27}\,{\rm cm}} = 2.67z^{0.95} + 49.36z^{1.65} - 29.88z^{2.0}. \tag{10}$$

Figure 1 shows the fit result. This formula agrees with observational data very well. The reduced χ^2 is 1.13. We apply this formula to GRBs whose redshifts are smaller than 1.40 in the sample of 69 GRBs (Schaefer 2007). After the luminosity $d_{\rm L}$ is obtained, the isotropic energy of GRB is calculated by $E_{\rm iso} = 4\pi d_{\rm L}^2 S_{\rm bolo}(1 + z)^{-1}$, where $S_{\rm bolo}$ is the bolometric fluence. The isotropic luminosity is $L_{\rm iso} = 4\pi d_{\rm L}^2 P_{\rm bolo}$, where $P_{\rm bolo}$ is the bolometric flux. Then the relations of $\tau_{\rm lag} - L$, $V - L$, $E_{\rm peak} - L$, $E_{\rm peak} - E_\gamma$, and $\tau_{\rm RT} - L$ can be fitted in $z < 1.40$. Here, the time lag ($\tau_{\rm lag}$) is the time shift between hard and soft light curves, L is the luminosity of a GRB, the variability V of a burst denotes whether its light curve is spiky or smooth and V can be obtained by calculating the normalized variance of an observed light curve around a smoothed version of that light curve (Fenimore & Ramirez- Ruiz 2000), $E_{\rm peak}$ is the peak energy in the νF_ν spectrum, $E_\gamma = (1 - \cos\theta_j)E_{\rm iso}$ is the collimation-corrected energy of a

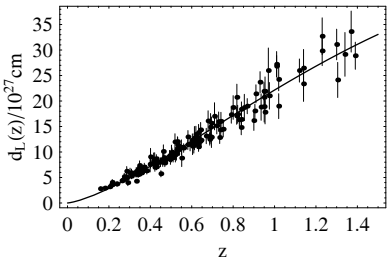

Fig. 1 Fitting the redshift z and luminosity distance $d_{\rm L}$. The line shows the formula of Eq. (10).

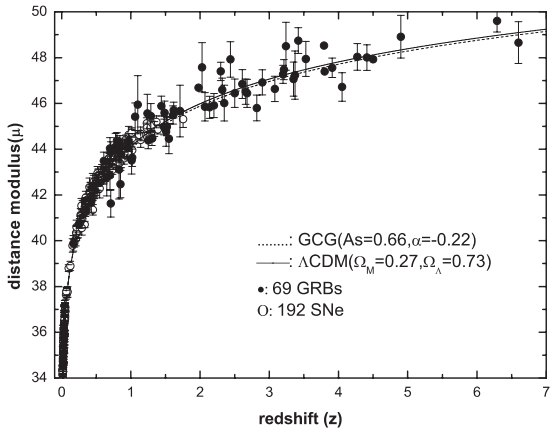

Fig. 2 Hubble diagram of 69 GRBs calibrated with SNe Ia and 192 SNe Ia. The solid line is plotted in a flat cosmology: Ω_M = 0.27 and Ω_Λ = 0.73. The dashed line is plotted in the GCG model: $A_s = 0.66$ and $\alpha = 0.22$.

GRB, and the minimum rise time ($\tau_{\rm RT}$) in the gamma-ray light curve is the shortest time over which the light curve rises by half of the peak flux of the pulse.

We assume that these relations do not evolve with redshift and are valid in $z > 1.40$. The luminosity or energy of GRB can be calculated. So, the luminosity distances and distance moduli can be obtained. After obtaining the distance modulus of each burst using one of these relations, we use the same method as Schaefer (2007) to calculate the real distance modulus,

$$\mu_{\rm fit} = \Big(\sum_i \mu_i/\sigma_{\mu_i}^2\Big)/\Big(\sum_i \sigma_{\mu_i}^{-2}\Big)\,, \tag{11}$$

where the summation runs from $1-5$ over the relations with available data, μ_i is the best estimated distance modulus from the i-th relation, and σ_{μ_i} is the corresponding uncertainty. The uncertainty of the distance modulus for each burst is

$$\sigma_{\mu_{\rm fit}} = \Big(\sum_i \sigma_{\mu_i}^{-2}\Big)^{-1/2}\,. \tag{12}$$

We present the Hubble diagram of 69 GRBs and 192 SNe Ia in Figure 2. We can see GRBs can extend the Hubble diagram to higher redshifts ($z > 6$). The GRB Hubble diagram is well behaved and delineates the shape of the Hubble diagram well. Liang et al. (2008) calibrated the luminosity relations of GRBs using an interpolation method. We find that our results are consistent with those calibrations by using interpolation methods. Kodama et al. (2008) also used SNe Ia to calibrate the $L - E_{\rm peak}$ relation.

3.2 Type Ia Supernovae (SNe Ia)

Davis et al. (2007) used the SN Ia dataset that includes 60 ESSENCE SNe Ia (Wood-Vasey et al. 2007), 57 SNe Ia from the Super-Nova Legacy Survey (SNLS) (Astier et al. 2006), 45 nearby SNe Ia and 30 SNe Ia detected by HST (Riess et al. 2007). We also use these 192 SNe Ia in this paper. The apparent magnitude $m(z)$ is related to the luminosity distance

$$m_{\rm th}(z) = \bar{M}(M, H_0) + 5\log_{10}(D_{\rm L}(z)) \tag{13}$$

where $D_{\rm L}(z) = H_0 d_{\rm L}(z)/c$ is the Hubble-free luminosity distance and

$$\bar{M} = M + 5\log_{10}\left(\frac{cH_0^{-1}}{\rm Mpc}\right) + 25 = M - 5\log_{10} h + 42.38 \tag{14}$$

is the magnitude zero point offset. The absolute magnitude M is assumed to be constant after implementing a correction for galactic extinction, K-correction and light curve width-luminosity correction. The theoretical distance modulus is

$$\mu_{\rm th}(z) = m_{\rm th}(z) + \mu_0, \tag{15}$$

where $\mu_0 = 42.38 - 5\log_{10} h$. The observed distance modulus is

$$\mu_{\rm obs}(z) = m_{\rm obs}(z) - M. \tag{16}$$

The likelihood functions can be determined from the χ^2 statistic,

$$\chi^2_{\rm SN} = \sum_{i=1}^{192} \frac{[\mu_{{\rm th},i}(z_i) - \mu_{{\rm obs},i}(z_i)]^2}{\sigma^2_{\mu_i}}, \tag{17}$$

where σ_{μ_i} is the uncertainty in the individual distance modulus. The parameter μ_0 is a nuisance parameter. The confidence regions can be found through marginalizing the likelihood functions over μ_0. The minimization with respect to μ_0 can be made by expanding the χ^2 of Equation (17) with respect to μ_0 as (Nesseris & Perivolaropoulos 2005; Perivolaropoulos 2005; Wei et al. 2007)

$$\chi^2(A_s, \alpha) = \bar{A} - 2\mu_0\bar{B} + \mu_0^2\bar{C}, \tag{18}$$

where

$$\bar{A}(A_s, \alpha) = \sum_{i=1}^{192} \frac{[m_{\rm obs}(z_i) - m_{\rm th}(z_i; \mu_0 = 0, A_s, \alpha)]^2}{\sigma^2_{m_{\rm obs}(z_i)}}, \tag{19}$$

$$\bar{B}(A_s, \alpha) = \sum_{i=1}^{192} \frac{[m_{\rm obs}(z_i) - m_{\rm th}(z_i; \mu_0 = 0, A_s, \alpha)]}{\sigma^2_{m_{\rm obs}(z_i)}}, \tag{20}$$

$$\bar{C} = \sum_{i=1}^{192} \frac{1}{\sigma^2_{m_{\rm obs}(z_i)}}. \tag{21}$$

Equation (18) has a minimum for $\mu_0 = \bar{B}/\bar{C}$ at

$$\tilde{\chi}^2(A_s, \alpha) = \bar{A}(A_s, \alpha) - \frac{\bar{B}^2(A_s, \alpha)}{\bar{C}}. \tag{22}$$

We can minimize $\tilde{\chi}^2$ which is independent of μ_0 instead of χ^2, because of $\chi^2_{\rm min} = \tilde{\chi}^2_{\rm min}$.

3.3 Cosmic Microwave Background (CMB)

The CMB shift parameter R is expected to be nearly model independent, which can be extracted accurately from CMB data. We make use of the 5-year WMAP results to get the shift parameter (Komatsu et al. 2008)

$$R = \sqrt{\Omega_M} \int_0^{z_{\rm ls}} \frac{dz}{E(z)} = 1.710 \pm 0.019\,, \tag{23}$$

where $E(z) \equiv H(z)/H_0$ is given in Equation (8), the last scattering redshift $z_{\rm ls} = 1089$ and $\Omega_M = \Omega_{\rm b} + (1-\Omega_{\rm b})(1-A_s)^{1/(1+\alpha)}$ (Zhu 2004; Bento et al. 2004). The χ^2 value is

$$\chi^2_{\rm CMB} = \frac{(R-1.710)^2}{0.019^2}\,. \tag{24}$$

3.4 X-ray Gas Mass Fraction in Clusters

The gas mass fraction of clusters of galaxies, $f_{\rm gas} = M_{\rm gas}/M_{\rm tot}$, as inferred from X-ray observations, can provide a direct constraint on the density parameter of the universe Ω_M (White et al. 1993). Using *Chandra* observational data, Allen et al. (2004) obtained the $f_{\rm gas}$ profiles for 26 relaxed clusters. This database has also been used to constrain the GCG model (Zhu 2004) and the braneworld cosmology (Zhu & Alcaniz 2005). We will utilize this probe in our analysis. Allen et al. (2008) recently presented the X-ray gas mass fraction in 42 hot dynamically relaxed galaxy clusters. The model fitting to the data is

$$f_{\rm gas}^{\Lambda{\rm CDM}} = \frac{K\tilde{A}\gamma b(z)}{1+s(z)} \frac{\Omega_{\rm b}}{\Omega_M} \left[\frac{d_{\rm A}^{\Lambda{\rm CDM}}(z)}{d_{\rm A}(z)}\right]^{1.5}\,, \tag{25}$$

where d_A is the angular diameter distance to the galaxy cluster, $\tilde{A} = (\frac{\theta_{2500}^{\Lambda{\rm CDM}}}{\theta_{2500}})^{\eta}$ accounts for the change in angle subtended by r_{2500} as the cosmology is varied, and η is the slope of the $f_{\rm gas}$ in the region of r_{2500} measured with reference to the ΛCDM model. The parameter γ denotes non-thermal pressure support in the clusters. The parameter $s(z) = s_0(1+\alpha_s z)$ shows the baryonic mass fraction in stars. The factor K is a constant that parameterizes residual uncertainty in the accuracy of instrument calibration and X-ray modeling. The factor $b(z) = b_0(1+\alpha_{\rm bz})$ is the 'depletion' or 'bias' factor (for more details see Allen et al. 2008). We calculate the χ^2 value as

$$\begin{aligned}\chi^2_{\rm gas} \;=\; & \left(\sum_{i=1}^{42} \frac{\left[f_{\rm gas}^{\Lambda{\rm CDM}}(z_i) - f_{{\rm gas},i}\right]^2}{\sigma^2_{f_{{\rm gas},\,i}}}\right) + \left(\frac{\Omega_{\rm b}h^2 - 0.0214}{0.0020}\right)^2 + \left(\frac{h-0.72}{0.08}\right)^2 \\ & + \left(\frac{s_0 - 0.16}{0.048}\right)^2 + \left(\frac{\eta - 0.214}{0.022}\right)^2 + \left(\frac{K-1.0}{0.1}\right)^2\,. \end{aligned} \tag{26}$$

4 CONSTRAINTS ON THE GCG MODEL

Using datasets of the above observational techniques, we measure constraints on the GCG model parameters A_s and α. We obtain the best fit by minimizing

$$\chi^2_{\rm total} = \chi^2_{\rm SN} + \chi^2_{\rm GRB} + \chi^2_{\rm CMB} + \chi^2_{\rm gas}\,. \tag{27}$$

In Figure 3, we show the 1σ to 3σ contours in the A_s-α plane using SNe, GRBs, the CMB shift parameter and 42 galaxy clusters. It is easy to see that ΛCDM still lies at the 2σ confidence level. From this figure, we have $A_s = 0.68^{+0.04}_{-0.08}$ and $\alpha = -0.22^{+0.15}_{-0.13}$ at the 1σ confidence level with $\chi^2_{\rm min} = 332.62$. We can rule out the standard Chaplygin gas model (α = 1) at the 3σ confidence level.

We also investigate the deceleration parameter $q(z)$. In Figure 4, we show the evolution of $q(z)$ in the GCG model using SNe, GRBs, the CMB shift parameter and 42 galaxy clusters. We obtain that the

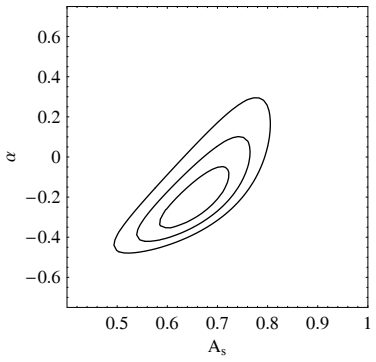

Fig. 3 Joint confidence intervals from 1σ to 3σ (A_s, α) derived from a combination of 192 SNe Ia, 42 galaxy clusters, 69 GRBs and the CMB shift parameter.

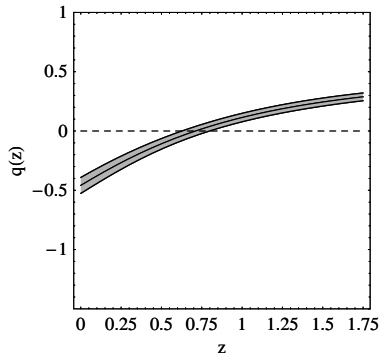

Fig. 4 Evolution of $q(z)$ by fitting the generalized Chaplygin gas model to 192 SNe Ia, 42 galaxy clusters, 69 GRBs and the CMB shift parameter. The solid line is plotted by using the best fitting parameters. The shaded region shows the 1σ error.

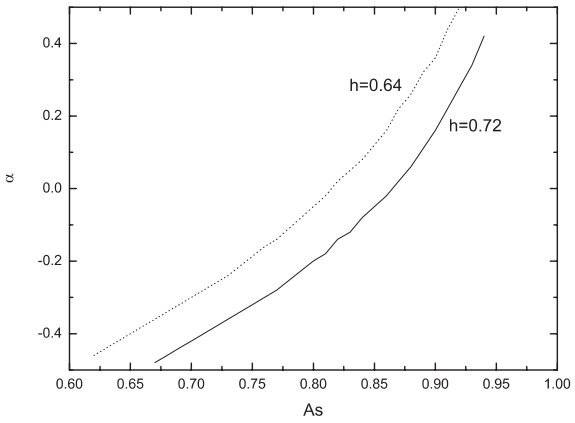

Fig. 5 The solid line is a contour for $t(3.91) = t_{\rm obs} = 2.0\,{\rm Gyr}$ with $h_0 = 0.72$. The dotted line is a contour for $t(3.91) = t_{\rm obs} = 2.0\,{\rm Gyr}$ with $h_0 = 0.64$. The region below the lines is allowed.

transition redshift $z_{\rm T} = 0.74 \pm 0.09$ at the 1σ confidence level. The result is consistent with Wang & Dai (2006) and Melchiorri et al. (2007).

We test the GCG model with an old high redshift object. It is obvious that the universe cannot be younger than its constituents. The discovery of a quasar named APM 08279+5255 at $z = 3.91$ whose age is 2–3 Gyr has led to a serious "age crisis" (Hasinger et al. 2002). This old quasar cannot be accommodated in many dark energy models (Jain & Dev 2006; Wei & Zhang 2007), even in the ΛCDM model. The age of the universe at redshift z is given by

$$t(z) = \frac{1}{H_0} \int_z^\infty \frac{dz'}{(1+z')H(z')}\,. \tag{28}$$

We use the most conservative lower age estimate of 2.0 Gyr for the old quasar APM 08279+5255 at $z = 3.91$. In Figure 5, we plot contours using $t(3.91) = t_{\rm obs} = 2.0\,{\rm Gyr}$. The allowed region is below the lines. We can see that the GCG model can overcome the serious "age crisis" (Alcaniz et al. 2003). For example, we take $A_s = 0.75$, $\alpha = -0.20$ and $h_0 = 0.64$, so that $t(3.91) = 2.00\,{\rm Gyr}$ is obtained.

The point ($A_s = 0.75, \alpha = -0.20$) is just on the dotted line. From Figures 3 and 5, we find that the old quasar APM 08279+5255 at $z = 3.91$ can be accommodated in the GCG model.

5 BREAKING THE DEGENERACY BETWEEN GCG AND XCDM MODELS

The GCG model and the XCDM model with equation of state $p/\rho = w$ and dark energy density $\Omega_X = 1 - \Omega_M$ are degenerate at redshifts $z < 2$, as shown in Bertolami et al. (2004), Bento et al. (2005) and Bertolami & Silva (2006). As we know, q is the deceleration parameter (which is related to the second derivative of the expansion factor), j is the so-called "jerk" or statefinder parameter (which is related to the third derivative of the expansion factor), and s is the so-called "snap" parameter (which is related to the fourth derivative of the expansion parameter). These quantities are defined by

$$q(t) = -\frac{1}{a}\frac{\mathrm{d}^2 a}{\mathrm{d}t^2}\left[\frac{1}{a}\frac{\mathrm{d}a}{\mathrm{d}t}\right]^{-2}; \tag{29}$$

$$j(t) = +\frac{1}{a}\frac{\mathrm{d}^3 a}{\mathrm{d}t^3}\left[\frac{1}{a}\frac{\mathrm{d}a}{\mathrm{d}t}\right]^{-3}; \tag{30}$$

$$s(t) = +\frac{1}{a}\frac{\mathrm{d}^4 a}{\mathrm{d}t^4}\left[\frac{1}{a}\frac{\mathrm{d}a}{\mathrm{d}t}\right]^{-4}. \tag{31}$$

The deceleration, jerk and snap parameters are dimensionless, and the Taylor expansion of the scale factor around t_0 provides

$$\begin{aligned} a(t) \;=\; & a_0\{1 + H_0(t-t_0) - \frac{1}{2}q_0 H_0^2 (t-t_0)^2 + \frac{1}{3!}j_0 H_0^3 (t-t_0)^3 \\ & + \frac{1}{4!}s_0 H_0^4 (t-t_0)^4 + O[(t-t_0)^5]\}, \end{aligned} \tag{32}$$

and so the luminosity distance

$$\begin{aligned} d_{\mathrm{L}} \;=\; & \frac{c}{H_0}\{z + \frac{1}{2}(1-q_0)z^2 - \frac{1}{6}(1 - q_0 - 3q_0^2 + j_0)z^3 \\ & + \frac{1}{24}[2 - 2q_0 - 15q_0^2 - 15q_0^3 + 5j_0 + 10q_0 j_0 + s_0]z^4 + O(z^5)\}, \end{aligned} \tag{33}$$

(Visser 2004). The relations between these parameters are given by (also see Bertolami & Silva 2006)

$$j(z) = q(z) + 2q^2(z) + (1+z)\frac{\mathrm{d}q(z)}{\mathrm{d}z}; \tag{34}$$

$$s(z) = -(1+z)\frac{\mathrm{d}j(z)}{\mathrm{d}z} - 2j(z) - 3j(z)q(z). \tag{35}$$

For the XCDM model, we obtain

$$q_0^{\mathrm{XCDM}} = \frac{3}{2}\left[1 + w(1-\Omega_M)\right] - 1, \tag{36}$$

$$\left.\frac{\mathrm{d}q}{\mathrm{d}z}\right|_0^{\mathrm{XCDM}} = \frac{9}{2}w^2(1-\Omega_M)\Omega_M, \tag{37}$$

$$\left.\frac{\mathrm{d}j}{\mathrm{d}z}\right|_0^{\mathrm{XCDM}} = -\frac{27}{2}w^2(1+w)(\Omega_M - 1)\Omega_M, \tag{38}$$

$$j_0^{\mathrm{XCDM}} = \frac{1}{2}[2 + 9(1-\Omega_M)w + 9(1-\Omega_M)w^2], \tag{39}$$

$$s_0^{\rm XCDM} = \frac{1}{4}[-14 - 81(1-\Omega_M)w - 9(16 - 19\Omega_M + 3\Omega_M^2)w^2 - 27(3 - 4\Omega_M + \Omega_M^2)w^3]. \quad (40)$$

For the GCG model we obtain

$$q_0^{\rm GCG} = \frac{3}{2}(1 - A_s) - 1 \quad (41)$$

$$\left.\frac{q}{{\rm d}z}\right|_0^{\rm GCG} = \frac{9}{2}A_s(1 - A_s)(1 + \alpha), \quad (42)$$

$$\left.\frac{{\rm d}j}{{\rm d}z}\right|_0^{\rm GCG} = -\frac{27}{2}\alpha(1+\alpha)(2A_s - 1)\,(A_s - 1)\,A_s, \quad (43)$$

$$j_0^{\rm GCG} = \frac{3}{4}(1 - A_s)[1 + (3 + 6\alpha)A_s], \quad (44)$$

$$s_0^{\rm GCG} = \frac{3}{8}(A_s - 1)[7 + 6(2 + \alpha - 6\alpha^2)A_s + 9(-3 + 2\alpha + 8\alpha^2)A_s^2]. \quad (45)$$

For the redshift range of SNe Ia, the terms beyond the cubic power in redshift in Equation (33) can be neglected. SN Ia data show that these models have the same deceleration and jerk parameters. So, they are degenerate in the SN Ia redshift range.

In Figure 6, we show constraints on Ω_M and w in the XCDM model. The solid contour, the dotted contour and the dot-dashed contour show constraints from 192 SNe, 69 GRBs and 192 SNe plus 69 GRBs, respectively. In Figure 7, we present constraints on A_s and α in the GCG model. From the solid contours, we measure $\Omega_M = 0.30 \pm 0.14, w = -1.09^{+0.35}_{-0.60}$ from Figure 6 and $A_s = 0.80^{+0.15}_{-0.13}, \alpha = 0.19^{+1.68}_{-0.87}$ from Figure 7. So $q_0^{\rm XCDM} = -0.62$, $j_0^{\rm XCDM} = 1.13$ and $q_0^{\rm GCG} = -0.68$, $j_0^{\rm GCG} = 1.19$ are calculated. We can see the degeneracy between the GCG model and XCDM model using SNe Ia only.

This degeneracy holds for SNe Ia for the probed maximum redshift $z \approx 2$. As the redshift range allowed by GRBs is greater ($z > 6.0$), we can measure higher order terms in Equation (33). From the dash-dotted contours of Figure 6, $\Omega_M = 0.29^{+0.11}_{-0.14}$ and $w = -1.04^{+0.32}_{-0.52}$ are found. From the dash-dotted contours of Figure 7, $A_s = 0.79^{+0.12}_{-0.13}$ and $\alpha = 0.25^{+0.95}_{-0.75}$ are found. For the XCDM model, we calculate $s_0^{\rm XCDM} = -0.08$. For the GCG model, we obtain $s_0^{\rm GCG} = -0.38$. So, the degeneracy between the models is broken by the snap parameter.

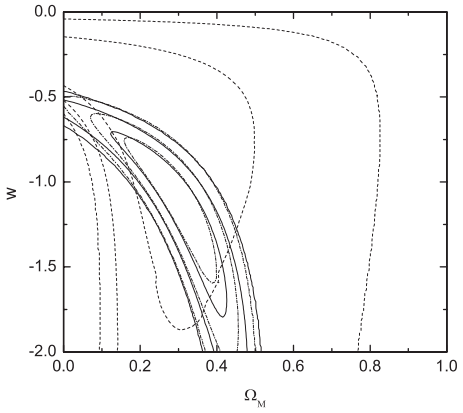

Fig. 6 Constraints on Ω_M and w from 1σ to 3σ using 192 SNe Ia and 69 GRBs in the XCDM model. The solid contour is derived from 192 SNe Ia alone and the dashed contour is derived from 69 GRBs. The dash-dotted contour is derived from 192 SNe Ia and 69 GRBs.

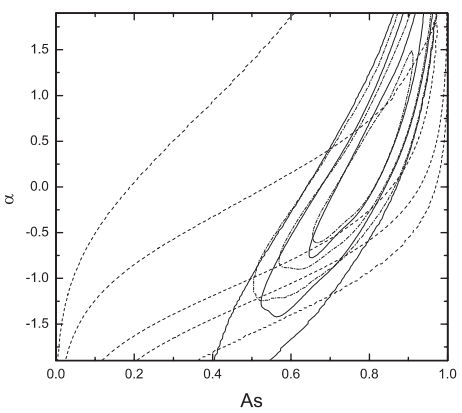

Fig. 7 Constraints on Ω_M and w from 1σ to 3σ using 192 SNe Ia and 69 GRBs in the GCG model. The solid contour is derived from 192 SNe Ia alone and the dashed contour is derived from the 69 GRBs. The dash dotted contour is derived from 192 SNe Ia and 69 GRBs.

6 CONCLUSIONS

In this paper, we calibrate the GRB luminosity relations without assuming any cosmological models using SNe Ia and find that GRB can extend the Hubble diagram to higher redshifts. We have presented constraints on the GCG model that unifies dark energy and dark matter in a single component by combining a recent GRB sample which includes 69 events with 192 SNe Ia, CMB and the X-ray gas mass fraction in clusters released recently. We found that $A_s = 0.68^{+0.04}_{-0.08}$ and $\alpha = -0.22^{+0.15}_{-0.13}$ at the 1σ confidence level using all the datasets. We reconstructed the deceleration parameter $q(z)$. We found that the cosmic acceleration could have started at about $z_{\rm T} \sim 0.70$. We find concordance of the GCG model with the age estimates of old quasar APM 08279+5255, although such a concordance cannot be accommodated in many dark energy models, even in the ΛCDM model. The degeneracy between the GCG model and XCDM model is broken by the snap parameter using the high redshift GRB sample.

Our present study shows that the GCG model is a very good fit to the latest datasets. The ΛCDM is allowed at the 2σ confidence level, but the standard Chaplygin gas model ($\alpha = 1$) is ruled out at the 3σ confidence level. Furthermore, GRBs can be used to break the degeneracy between the GCG model and XCDM model, because at high redshifts, the effect of higher-order terms in the Taylor expansion of $d_{\rm L}(z)$ must be taken into account. We break the degeneracy between the two models using the GRB sample. There are two mechanisms to drive acceleration in the present universe: modified gravity and dark energy. Our study suggests that GRBs may break the degeneracy between these two mechanisms.

In this paper, we first use 69 GRBs (five relations) to put constraints on the GCG model and extend the Hubble diagram out to $z > 6.0$. We show that the old quasar APM 08279+5255 can be accommodated in the GCG model even in the $\alpha < 0$ case. Alcaniz et al. (2003) found that there was no cosmic age problem in the GCG model when $\alpha > 0$. Bertolami & Silva (2005) used 500 simulated GRBs and the Ghirlanda relation to investigate the GCG model. They predicted that the *SNAP*+GRB data could break the degeneracy between the GCG model and the XCDM model. We break the degeneracy between these two models by combining the most recent GRB and SN Ia data.

Acknowledgements This work was supported by the National Natural Science Foundation of China (grants 10221001, 10640420144 and 10873009) and the National Basic Research Program of China (973 program) No. 2007CB815404. Fa-Yin Wang was also supported by the Jiangsu Project Innovation for PhD Candidates (CX07B-039z). Shi Qi was supported by the Scientific Research Foundation of Graduate School of Nanjing University.

References

Alcaniz, J. S., Jain, D., & Dev, A. 2003, Phys. Rev. D, 67, 043514
Allen, S. W., et al. 2004, MNRAS, 353, 457
Allen, S. W., et al. 2008, MNRAS, 383, 879
Astier, P., et al. 2006, A&A, 447, 31
Basilakos, S., & Perivolaropoulos, L. arXiv:0805.0875v1
Bennett, C. L., et al. 2003, ApJS, 148, 97
Bento, M. C., Bertolami, O., & Sen, A. A. 2002, Phys. Rev. D, 66, 043507
Bento, M. C., Bertolami, O., & Sen, A. A. 2003, Phys. Lett. B, 575, 172
Bento, M. C., Bertolami, O., & Sen, A. A. 2004, Phys. Rev. D, 70, 083519
Bento, M. C., Bertolami, O., Santos, N. M. C., & Sen, A. A. 2005, Phys. Rev. D, 71,063501
Bertolami, O., Sen, A. A., Sen, S. & Silva, P. T. 2004, MNRAS, 353, 329
Bertolami, O. & Silva, P. T. 2006, MNRAS, 356, 1149
Caldwell, R. R., Dave, R., & Steinhardt, P. J. 1998, Phys. Rev. Lett., 80, 1582
Cohen, A., Kaplan, D., & Nelson, A. 1999, Phys. Rev. Lett., 82, 4971
Dai, Z. G., Liang, E. W., & Xu, D. 2004, ApJ, 612, L101
Davis, T. M., et al. 2007, ApJ, 666, 716
Deffayet, C, Dvali, G. R., & Gabadadze, G. 2002, Phys. Rev. D, 65, 044023
Dev, A., Jain, D., & Alcaniz, J. S. 2003, Phys. Rev. D, 67, 023515

Di Girolamo, T., et al. 2005, JCAP, 4, 008
Dvali, G. R., Gabadadze, G., & Porrati, M. 2000, Phys. Lett. B, 485, 208
Firmani, C., Ghisellini, G., Ghirlanda, G., & Avila-Reese, V. 2005, MNRAS, 360, L1
Fenimore, E. E., & Ramirez-Ruiz, E. 2000, astro-ph/0004176
Freedman, W., et al. 2001, ApJ. 553, 47
Friedmann, A. S., & Bloom, J. S. 2005, ApJ, 627, 1
Ghirlanda, G., et al. 2004, ApJ, 613, L13
Gong, Y., & Chen, X. L. arXiv: 0708.2977v2
Gong, Y., & Duan, C. K. 2004, Class. Quant. Grav, 21, 3655
Guo, Z. K., & Zhang, Y. Z. 2007, Phys. Lett. B, 645, 326
Hasinger, G., et al. 2002, ApJ, 573, L77
Jain, D., & Dev, A. 2006, Phys. Lett. B, 633, 436
Kamenshchik, A., Moschella, U., & Pasquier, V. 2001, Phys. Lett. B, 511, 265
Kirkman, D., et al. 2003, ApJS, 149, 1
Kodama, Y., et al. arXiv: 0802.3428v2
Komatsu, E., et al. 2009, ApJS, 180, 330
Lamb, D. Q., et al. 2005, astro-ph/0507362
Li, H., et al. arXiv: 0711.0792
Li, H., et al. 2008, Phys. Lett. B, 658, 95
Li, M. 2004, Phys. Lett. B, 603, 1
Liang, E. W., & Zhang, B. 2005, ApJ, 633, 611
Liang, E. W., & Zhang, B. 2006, MNRAS, 369, L37
Liang, N., et al. arXiv: 0802.4262v4
Makler, M., de Oliveira, S. Q., & Waga, I. 2003, Phys. Lett. B, 555, 1
Melchiorri, A., et al. 2007, Phys. Rev. D, 76, 041301
Möller, P., et al. 2002, A&A, 396, L21
Mortsell, E., & Sollerman, J. 2005, JCAP, 0506, 009
Multamaki, T., Manera, M., & Gaztanaga, E. 2004, Phys. Rev. D, 69, 023004
Nesseris, S., & Perivolaropoulos, L. 2005, Phys. Rev. D, 72, 123519
Perivolaropoulos, L. 2005, Phys. Rev. D, 71, 063503
Perlmutter, S., et al. 1999, ApJ, 517, 565
Peebles, P. J. E., & Ratra, B. 2003, Rev. Mod. Phys. 75, 559
Qi, S., Wang, F. Y., & Lu, T. 2008a, A&A, 483, 49
Qi, S., Wang, F. Y., & Lu, T. 2008b, A&A, 487, 853
Ratra, B., & Peebles, P. J. E. 1988, Phys. Rev. D, 37 3406
Riess, A. G., et al. 1998, AJ, 116, 1009
Riess, A. G., et al. 2007, ApJ, 659, 98
Schaefer, B. E. 2007, ApJ, 660, 16
Silva, P. T., & Bertolami, O. 2003, ApJ. 599, 829
Spergel. D. N., et al. 2003, ApJS, 148, 175
Spergel. D. N., et al. 2007, ApJS, 170, 377
Su, M., Fan, Z. H., & Liu, B. 2006, astro-ph/0611155
Tegmark, M., et al. 2006, Phys. Rev. D., 74, 123507
Visser, M. 2004, Class. Quant. Grav., 21, 2603
Wang, F. Y., & Dai, Z. G. 2006, MNRAS, 368, 371
Wang, F. Y., Dai, Z. G., & Zhu, Z. H. 2007, ApJ, 667, 1
Wei, H., Tang, N. N., & Zhang, S. N. 2007, Phys. Rev. D, 75, 043009
Wei, H., & Zhang, S. N. 2007, Phys. Rev. D, 76, 063003
Weinberg, S. 1989, Rev. Mod. Phys, 61, 1
Wetterich, C. 1988, Nucl. Phys. B, 302, 668
White, S. D. M., et al. 1993, Nature, 366, 429
Wood-Vasey, W. M., et al. 2007, ApJ, 666, 694
Wright, E. L. 2007, ApJ, 664, 633
Wu. P. X., & Yu, H. W. 2007, JCAP, 03, 015
Xu, D., Dai, Z. G., & Liang. E. W. 2005, ApJ, 633, 603
Zhang, H., & Zhu, Z.-H. 2006, Phys. Rev. D, 73, 043518
Zhu, Z.-H. 2004, A&A, 423, 421
Zhu, Z.-H., & Alcaniz, J. S. 2005, ApJ, 620, 7
Zhu, Z.-H., & Fujimoto, M. 2002, ApJ, 581, 1